Supplementory information

Paracrine WNT5A signaling inhibits expansion of tumor-initiating cells

Authors: Nicholas Borcherding[1,2,10], David Kusner[1,3,10], Ryan Kolb[1,4,10], Qing Xie[1,7], Wei Li[1], Fang Yuan[1,8], Gabriel Velez[2], Ryan Askeland[1,9], Ronald J. Weigel[5,6], Weizhou Zhang[1,2,3,4,6]

[1]Department of Pathology

[2]Medical Science Training Program

[3]Molecular and Cellular Biology Program

[4]Immunology Program

[5]Department of Surgery

[6]Holden Comprehensive Cancer Center

University of Iowa, College of Medicine

Iowa City, IA 52242-1109

[7]College of Veterinary Medicine, Nanjing Agricultural University, China

[8]Department of Nephrology, The Second Xiangya Hospital, Central South University, Changsha, Hunan 410011, P.R. China

[9]Current address: University of South Dakota Sanford School of Medicine, Sioux Falls, SD 75105

[10]These authors contributed equally to this work.

Correspondence: weizhou-zhang@uiowa.edu (WZ)

Running Title: Tumor suppressive effect of WNT5A on breast cancer.

Supplementary Information

Supplenmentary Methods:

RNA Isolation from Basal and Luminal TIC-Formed Tumors and Mouse Illumina Array

Tumors were generated from our previous study where different mammary epithelial cells from pre-neoplastic mammary glands of 5-month-old *MMTV-ErbB2* female mice were injected into a mammary fat pad of female mice (1). 20 mg of tumor was homogenized and RNA was isolated using the RNeasy Plus mini kit (QIAGEN, Venlo, Limburg, Netherlands). RNA quality was assessed by Agilent 2100 Bioanalyzer. 100 ng of RNA was submitted to the Genomics Division of the University of Iowa for cDNA synthesis and *in vitro* transcription, converting RNA to Biotin-aRNA using the Epicentre Target AMP-Nano labeling Kit (Illumina San Diego, CA). Converted Biotin-aRNA was purified with RNeasy MinElute cleanup column (QIAGEN) according to the instruction by Epicentre. In Illumina hybridization buffer, 750 ng of Biotin-aRNA were placed onto Illumina Mouse WG-6 v2.0 Beadchip (Illumina) at 58° C for 17 h with oscillation. Succeeding hybridization, the arrays were washed, blocked with Illumina Direct Hybridization Kit, and stained with streptavidin-Cy3 (Amersham/GE Healthcare, Piscataway, NJ) according to Illumina Direct Hybridization Assay protocols. Beadchips were assayed with the Illumina iScan System and data was collected using GenomeStudio software v2011.1.

We confirmed 13 upregulated genes and 11 downregulated genes using quantitative real-time PCR analysis and here are the lists for primers, using PPIA as the house keeping gene:

Downregulated	**5'-3' sequences**		**Upregulated**	**5'-3' sequences**
mGPRASP2-F	TGCCACTCATCAGCCTTATG		mDMRT3-F	GAGCTCCTCTGATCGGTGTC
mGPRASP2-R	AAGAGATTGACAAGTTAAC		mDMRT3-R	AGCGCAGCTTGCTAAACCAG
mOLFML3-F	CAGCATGCCGACTACTCTGA		mANGPT2-F	TCTGGTTCTGCACCACATTC
mOLFML3-R	CAGCACCACCTTGTGGAGTA		mANGPT2-R	ACAACACACAGTGGCTGATGA
mCSN2-F	CAAGAGCAAGGGCCACAAG		mIDH2-F	CACCGTCCATCTCCACTACC
mCSN2-R	TCCTTTCAGCTTCACCTCCT		mIDH2-R	CAGCACTGACTGTCCCCAG
mWNT5A-F	AACTTGGAAGACATGGCACC		mYWHAZ-F	GAAGCATTGGGGATCAAGAA
mWnt5A-R	ACGCTTCGCTTGAATTCCT		mYWHAZ-R	CAGCAGATGGCTCGAGAATA
mCPSF4L-F	AACAGGCATTCCTTGTTGCT		mTNFRSF19-F	CTGGAGACGGTGGAGGAGAT
mCPSF4L-R	AGTGATTGCTGCGACTTCCT		mTNFRSF19-R	CAAGACATGGAGTGTGTGCC
mLY6D-F	GGCAGACCTGAGGGTTCTTA		mDNMT3B-F	CTGGCACCCTCTTCTTCATT

mLY6D-R	CTCTGCTCGTCCTCCTTGTC		mDNMT3B-R	ATCCATAGTGCCTTGGGACC
mSMOC1-F	AGTCCTGGGACAGTGTGGGT		mPIK3R3-F	GCTGGAGTCATTGGCTTAGG
mSMOC1-R	CTGCTCGTGTTGGTGCAG		mPIK3R3-R	TGATGATGCCCTATTCGACA
mMFGE8-F	AGATGTCATTGTCTTGGCCC		mMMP12-F	TTTGGATTATTGGAATGCTGC
mMFGE8-R	ATGCTACTCTGCGCCTCTG		mMMP12-R	ATGAGGCAGAAACGTGGACT
mFBLN2-F	AGAGCTGTGACCAGAGCCAA		mPDK1-F	TTACTCAGTGGAACACCGCC
mFBLN2-R	GCAGCTCAACACAGAGCACC		mPDK1-R	GTTTATCCCCCGATTCAGGT
mGPR77-F	CTGGTGGTGTGGTTCATCAT		mIGF1-F	CACTCATCCACAATGCCTGT
mGPR77-R	GCTCACATCCAGGAAGCTGT		mIGF1-R	TGGATGCTCTTCAGTTCGTG
mCD177-F	CCGGGAGAATATGGAGACAC		mPDGFa-F	CCTCACCTGGACCTCTTTCA
mCD177-R	CGCTGCTGCTCATAGACGTA		mPDGFa-R	TAACACCAGCAGCGTCAAGT
			mANGPTL4-F	GGAAAAGTCCACTGTGCCTC
House keeping			mANGPTL4-R	TTTCCAAGATGACCCAGCTC
mPPIA-F	CAGTGCTCAGAGCTCGAAAGT		mCTGF-F	CCGCAGAACTTAGCCCTGTA
mPPIA-R	GTGTTCTTCGACATCACGGC		mCTGF-R	AGCTGACCTGGAGGAAAACA

Quantitative PCR

RNA was isolated using RNeasy Mini Plus kit (QIAGEN) and reverse-transcribed with iScript cDNA Synthesis Kit (Bio-Rad) or SuperScript RT III (Life Technologies). PCR was performed with iTaq Universal SYBR Green Supermix (Bio-Rad) in a 15 µl reaction volume. Primers used were: cyclin D1 forward primer: 5'-GCT GCG AAG TGG AAA CCA TC-3' and reverse primer: 5'-CCT CCT TCT GCA CAC ATT TGA A-3'; CTNNB1 forward primer: 5'-CCT CAG ATG GTG TCT GCT ATT G-3' and reverse primer: 5'-CCT TCC ATC CCT TCC TGT TTA G-3'; BCL-XL forward primer: 5'-GAG CTG GTG GTT GAC TTT CT-3' and reverse primer: 5'-TGG TCA GTG TCT GGT CAT TTC-3'; GATA3 forward primer: 5'-GAG GGA GAG AGA GAG AGA AGA A-3' and reverse primer: 5'-GGA AGC AAA GGT GAG CAA AG-3'; p15 forward primer: 5'-GAC CGG GAA TAA CCT TCC ATA C-3' and reverse primer: 5'-CTC CAC TTT GTC CTC AGT CTT C-3'; p21 forward primer: 5'-GGA AGG GAC ACA CAA GAA GAA-3' and reverse primer: 5'-TCC TTG TTC CGC TGC TAA TC-3'. Real-time PCR was performed using the Vii7 machine (ABI, Life Technologies).

Separation of Mammary Epithelial cells and spheroid growth in matrigel

We followed previously established protocols (2). Briefly, mammary glands were sequentially digested with 300 µg/ml collagenase and 100 µg/ml hyaluronidase (Stemcell, Vancouver, BC, Canada), 0.25% trypsin-EDTA (Mediatech, Corning, NY) and 5 µg/ml dispase I (Stemcell) and 0.1 µg/ml DNase I (Worthington, Lakewood, NJ). Single cells were labeled with a cocktail of antibodies for flow cytometry to separate different epithelial cells using BD Aria II as illustrated (**Supplementary Fig. S2**). For spheroid growth on matrigel (BD Biosciences), 1000 cells were seeded onto matrigel-coated 8-well chamber slide (2), mock-treated, treated with 100 ng/ml of WNT5A (R&D Systems, Minneapolis, MN), or 100 ng/ml WNT5A together with 5 µM of SB-431542 (Stemgent, Cambridge, MA) **(3)**. Spheroids were photographed three weeks later as before **(1)** and the size was quantitated using *ImageJ* software **(4)**.

TCGA Analyses

The UCSC Cancer Genome Browser (https://genome-cancer.ucsc.edu) was used to assess copy number variations (CNV) across all available cancer datasets in the TCGA (25). Samples with GISTIC2 values of -1 or -2 were compared to the number of total patients. Expression analysis for the TCGA BRCA cohort were done using mean-centralized level 3 Illumina HiSeq 2000 RNAseq for primary tumor samples and GISTIC2 threshold method for copy number estimates. RNAseq expression data was transformed as log2(x+1) to prevent error for 0 values. Samples were divided into indicated categorical groups using the Biotab clinical information available at the TCGA DCC (https://tcga-data.nci.nih.gov/tcga/). Differences in sample numbers between figures were a result of sorting by categorical data, i.e. the number of primary tumor samples that have PAM50 subtypes are less than the total number of primary samples with RNAseq expression. Provisional overall survival data was used to generate survival curves using all available centralized level 3 Illumina HiSeq expression data for primary tumors. *WNT5A* expression VS. DNA methylation analysis was performed with mean-centralized level 3 Illumina HiSeq 2000 RNAseq expression data and Infinium HumanMethylation450 β-values of all 58 probes from the UCSC Cancer Genome Browser.

Supplementary Table 1

Gene ID	Average Log2 Change	P-value
GPRASP2	-3.31014	0.008416
CD177	-3.07961	0.046413
BC026585	-2.86871	0.014095
OLFML3	-2.63842	0.002424
CSN2	-2.557496667	0.019846
WNT5A	**-2.533973333**	**0.009711**
CPSF4L	-2.2381	0.017814
LY6D	-2.198563333	0.037358
HOXB2	-2.196153333	0.03495
CP	-2.17223	0.023444
LOC380706	-2.171803333	0.009343
LOC381957	-2.145343333	0.023889
SMOC1	-2.071853333	0.005773
MFGE8	-1.9999	0.010347
FBLN2	-1.953063333	0.015761
GM1673	-1.887533333	0.04665
GPR77	-1.771956667	0.018207
SCNN1G	-1.770906667	0.002349
SERPINA3H	-1.712306667	0.024589
DPYD	-1.706243333	0.042413
SCNN1B	-1.699393333	0.006045
AABP3-PENDING	-1.6878	0.041314
CASP4	-1.640403333	0.049816
CD200	-1.62606	0.023314
SLC38A3	-1.61648	0.022071
ANK	-1.605553333	0.004339
4933427D14RIK	-1.60026	0.017422

Gene ID	Average Log2 Change	P-value
GCNT1	1.58544	0.019437
BICC1	1.592483333	0.047655
RELL1	1.5937	0.039446
LOC626152	1.600913333	0.025303
PTPRA	1.629953333	0.041639
ST3GAL4	1.6327	0.014223
SCL0003799.1_2	1.639963333	0.024348
PNPLA3	1.644606667	0.022422
RNASE1	1.651023333	0.007171
PIK3R3	1.70152	0.013612
H1F0	1.704946667	0.041049
AKAP12	1.739686667	0.004597
ANKRD37	1.75697	0.008357
GLRX1	1.780666667	0.024041
PIP	1.791	0.000352
CHIT1	1.797913333	0.030088
ESM1	1.810673333	0.029836
DNMT3B	1.874343333	0.000914
OTX1	1.897516667	0.010942
LRP11	2.024416667	0.003859
ANGPT2	2.296486667	0.035011
ATP10B	2.373126667	0.003193
PSP	2.393066667	0.006228
4930533K18RIK	2.494036667	0.016075
PDLIM4	2.660586667	0.008894
RAB6B	2.691356667	0.033865
EG545886	3.1337	0.026646
DMRT3	3.829756667	0.01652

Note: Index of genes upregulated or downregulated in basal-TIC tumors relative to luminal-TIC tumors. Change was reported in log2.

Supplementary Table 2

	HER2	Lum A	LumB	BLBC
ΔHomo	1/1.5	2/0.5	1/0.5	1/0.7
ΔHet	33/49.3	74/17.9	71/37.0	80/59.2
Diploid	29/43.3	300/72.6	95/49.5	46/34.1
Gain	4/6.0	37/9.0	25/13.0	8/5.9
Total	67	413	192	135

WNT5A CNV by PAM50 molecular subtype from samples with both RNAseq expression data and CNV (n=807). ΔHomo, homozygous deletion; ΔHet, heterozygous deletion; Gain, increased copy number; Lum A, luminal A; Lum B, Luminal B; BLBC, basal-like breast cancer. Data were shown as number of cases/percentage of the PAM50 molecular subtypes.

Supplementary Legends:

Figure S1: Verification of Illumina Array by reverse transcription real-time PCR analysis (Supplementary for Figure 1). Total RNAs were purified from three-paired tumors derived from basal TICs and luminal TICs for real-time PCR analyses. Fold changes in gene expression between paired specimens were shown. 13 upregulated genes (**A**) or 11 downregulated genes (**B**) in basal TIC-formed tumors relative to luminal TIC-formed tumors were analyzed. Mouse 1-3 represent 3 tumor-pairs from 3 different mice. Red dotted lines in **A-B** represent the base gene expression (i.e. scale 1) from luminal TIC-formed tumors.

Figure S2: Allelic loss of *WNT5A* led to decreased WNT5A expression in human breast-cancer specimens and mouse luminal epithelial cells. A. *WNT5A* expression did not correlate with DNA methylation status in human breast-cancer specimens. *WNT5A* expression Vs. DNA methylation analysis was performed with mean-centralized level 3 Illumina HiSeq 2000 RNAseq expression data and Infinium HumanMethylation450 β-values from the UCSC Cancer Genome Browser. **a.** No correlation between *WNT5A* expression and the average of β-values from all 58 methylation probes. **b-f.** No correlation between *WNT5A* expression and β-values from 5 most variable probes in breast cancer subtypes. All specimens are categorized by PAM50. **B.** Heterozygous loss of *WNT5A* allele led to decreased mRNA expression in advance stage cancer specimens. The TCGA BCA dataset was downloaded and analyzed based on tumor stages (Stages 1-4). The expression of *WNT5A* mRNA was compared between cancer specimens with either diploid (D) or haploid (H) *WNT5A* locus. **C.** Heterozygous deletion of *WNT5A* resulted in decreased WNT5A expression in luminal mammary epithelial cells. Mouse mature luminal epithelial cells were purified from either wild type mice (WT LC) or *Wnt5a*$^{+/-}$ mice (*Wnt5a*$^{+/-}$ LC) and cultured. Conditioned medium (CM) were collected and further concentrated 10 times. Recombinant WNT5A protein at different concentrations (50-500 ng/ml, left panel) and 10-time concentrated

conditioned medium (right panels) were spotted onto nitrocellulose membrane, followed by immunoblotting with anti-WNT5A antibody.

Figure S3: Schematic depiction of the purification procedure for different populations of mammary epithelial cells. Briefly, mouse mammary glands were digested with collagenase and hyaluronidase following instruction from Stemcell to get organoids, which was further separated into single cells by Trypsin, Dispase I and DNase I. Cells were counted and labeled with a cocktail of antibodies with different fluorophores, followed by flow cytometry to eliminate cell aggregates, dead cells, and lineage-positive (CD45, CD31 and Ter119)$^{+}$ cells. The remaining cells were analyzed for expression of CD24, CD49f and CD61. P6 represents CD24^{low}CD49f^{high} basal cell population. P5 represents CD24^{high}CD49f^{low} luminal cells that can be further separated into CD61^{+} luminal progenitor cells and CD61^{-} mature luminal cells.

Figure S4: Supplementary information of Figure 4. A. Representative images for mammospheres from magnetically-purified pre-neoplastic *MMTV-ErbB2* mammary epithelial cells with or without 100 ng/ml of WNT5A supplement. **B.** Quantification of the resulting number of mammosphere efficiency from **A** (spheres per 1000 cells) (P = 0.001, n=3). **C.** Basal TICs were purified and seeded onto matrigel-coated chambers, either non-treated (NT), or treated with different doses of WNT5A (50, 100, or 200 ng/ml). Spheroids were counted and numbers were shown after 3 weeks. **D.** Basal and luminal TICs were purified from pre-neoplastic mammary glands of 5-month old *MMTV-ErbB2* female mice by flow cytometry and seeded onto matrigel-coated 8-well slide chambers, either mock treated or treated with 100 ng/mL of WNT5A or in combination with 5 μM of SB-431542. **E.** Basal and luminal TICs were purified and seeded onto matrigel-coated 8-well slide chambers, either alone or co-cultured with purified mature luminal cells (LC) from either WT or *Wnt5a*$^{+/-}$ female mice. After 3 weeks, spheroids were

photographed with representative images shown. Mature LCs from WT or *Wnt5a*$^{+/-}$ female mice do not form spheroids and were shown. **F.** Basal TICs and mature luminal cells from *Wnt5a*$^{fl/fl}$ females (*Wnt5a*$^{fl/fl}$ LC) were co-seeded onto matrigel at 1:5 ratio; 24 hrs later, cells were either treated with adenovirus encoding GFP (Adv-GFP) or Cre DNA recombinase (Adv-Cre). Basal TICs alone were also treated with Adv-GFP or Adv-Cre. *Wnt5a*$^{fl/fl}$ LC did not form spheroids under these conditions (*Wnt5a*$^{fl/fl}$ LC). After 3 weeks, spheroids were photographed with representative images shown. The right panels were immunoblots showing that 72 hrs of treatment with Adv-Cre completely deleted WNT5A expression in *Wnt5a*$^{fl/fl}$ LC. **G**. Basal TIC from pre-neoplastic MMTV-*ErbB2*-Tg female mice were purified and grown on matrigel for three weeks. Spheroids were embedded with OCT for frozen sections and immunostained with non-immune rabbit IgG and rat IgG (no staining observed, data not shown), or with anti-WNT5A and anti-keratin 8 (KRT8) antibodies, counterstained with DAPI. Representative hollow spheroid acinus (top panels) and solid spheroid (bottom panels) were shown.

Figure S5: Heterozygous deletion of *Wnt5a* has no impact on normal mammary gland development. **A.** Whole mount of #4 mammary fat pads from 12-week old WT or *Wnt5*$^{+/-}$ female littermates showing no obvious phenotypic difference. **B**. H & E staining of paraffin-embedded sections of either #2 or #4 mammary gland from 12-week old *ErbB2*/*WT* or *ErbB2*/*Wnt5*$^{+/-}$ female littermates showing no histological difference. n=3 littermates.

Figure S6: WNT5A induces the phosphorylation of SMAD2. A. HMLE cells were treated with WNT5A or WNT5A + TGFβR1 inhibitors SB-341542 (5 μM) for different periods. **B.** MCF10A cells were treated with WNT5A (100 ng/ml) or TGFβ (5 ng/ml) for 1 hr. 1, 2 and 3 represent samples from independent experiments. Protein band densitometry for p-SMAD2 was measured and normalized to total SMAD proteins. **C.** MDA-MB-231 cells were treated with WNT5A (100ng/ml) for the indicated periods. **D**. MCF10A cells were either untreated or treated with WNT5A, or together with two different TGFβR1

inhibitors SB-341542 (5 μM) or SB-505124 (1 μM). For **A-D**. Cell lysates were collected and separated by SDS-PAGE, followed by immunoblotting with the indicated antibodies. **E.** HMLE cells were treated with WNT5A (100 ng/ml) or TGFβ (5 ng/ml) for the indicated time periods. RNAs were collected, reverse-transcribed and subjected to real-time PCR analysis for Smad-targeted genes (n=3, *$P < 0.05$; ** $P < 0.01$; *** $P < 0.001$).

Figure S7: Differential expression of canonical and noncanonical Wnt receptors in basal and luminal epithelial cells. A-B. *RYK* expression is decreased in breast cancer. TCGA Illumina HiSeq level 3 expression of breast cancer dataset was downloaded and *RYK* expression was analyzed and compared between normal tissues and cancer specimens (**A**) ($P = 0.0154$, case numbers indicated), or compared between normal tissues with different types of breast cancer (**B) (**P-values were calculated with unpaired Welch's T-test for normal samples relative to Luminal A ($P < 0.0001$), Luminal B ($P < 0.0001$), HER2 ($P < 0.0001$), and BLBC ($P < 0.0011$). **C.** Microarray dataset GSE37223 deposited in GEO Datasets in Pubmed Central was downloaded and analyzed for the expression of Wnt receptors in $CD49f^{+}EPCAM^{-}$ human basal mammary epithelial cells and $CD49f^{-}EPCAM^{+}$ luminal epithelial cells (** $P \leq 0.0053$, *** $P = 0.005$, **** $P < 0.0001$, n=7). **D**. The frozen sections of human invasive cancer specimens and adjacent normal tissues were stained with with anti-RYK (Green) and anti-KRT8 (Red) antibodies. We stained spheroids from Supplementary Fig. S3D with non-immune rabbit IgG and rat IgG (no staining observed, bottom panels) as negative controls. Nuclei were counterstained with DAPI. Three paired normal mammary tissues and invasive breast cancer specimens were included. Representative pictures were shown.

Figure S8: *RYK* or *SMAD2* expression does not correlate with metastasis-free survival. A. MCF10A parental cells, or MCF10A cells expressing *RYK* shRNA1 or shRNA2 used in **Figure 7A** were cultured and either left untreated (NT) or treated with WNT5A (100 ng/ml) or TGFβ (5 ng/ml).

Cell lysates were collected, separated by SDS-PAGE and immunoblotted with the indicated antibodies. **B-C.** MCF10A cells expressing control luciferase shRNA, *RYK* shRNA1 or shRNA2 were cultured under matrigel. One week later, spheroids were formed and photographed. Spheroid size was calculated with *ImageJ*. Representative images were shown (**B**) and summarized (**C**). n=23-40 from 2 independent experiments (**, P <0.01). **D-F.** The 255 specimens from GSE2034 were equally separated into 4 groups based on *RYK* or *SMAD2* expression. The correlation between metastasis-free survival and *RYK* (**D**) or *SMAD2* (**E**) expression was analyzed and Kaplan-Meier curve was graphed using Prism 6 software. *P* values and case numbers are indicated in the plot. **F.** 255 specimens in GSE2034 were separated to four groups based on the expression level of *RYK* and *SMAD2*. Low (assigned as 0) and high (assigned as 1) expression of *RYK* or *SMAD2* were defined as expression values lower or higher than median values. N numbers and *P* value comparing 1/1 group VS. 0.0 group is indicated. The correlation between metastasis-free survival and *RYK/SMAD2* expression was analyzed and Kaplan-Meier curve was graphed using Prism 6 software.

Figure S9: Schematic depiction of the major conclusions and explained in detail in the Discussion section.

Supplementary References:

1. Zhang W, Tan W, Wu X, Poustovoitov M, Strasner A, Li W, et al. A NIK-IKKα Module Expands ErbB2-Induced Tumor-Initiating Cells by Stimulating Nuclear Export of p27/Kip1. Cancer Cell 2013;23(5):647-59.
2. Debnath J, Muthuswamy SK, Brugge JS. Morphogenesis and oncogenesis of MCF-10A mammary epithelial acini grown in three-dimensional basement membrane cultures. Methods 2003;30(3):256-68.
3. Mroue R, Bissell MJ. Three-dimensional cultures of mouse mammary epithelial cells. Methods in molecular biology 2013;945:221-50.
4. Schneider CA, Rasband WS, Eliceiri KW. NIH Image to ImageJ: 25 years of image analysis. Nat Meth 2012;9(7):671-75.

Figure S1

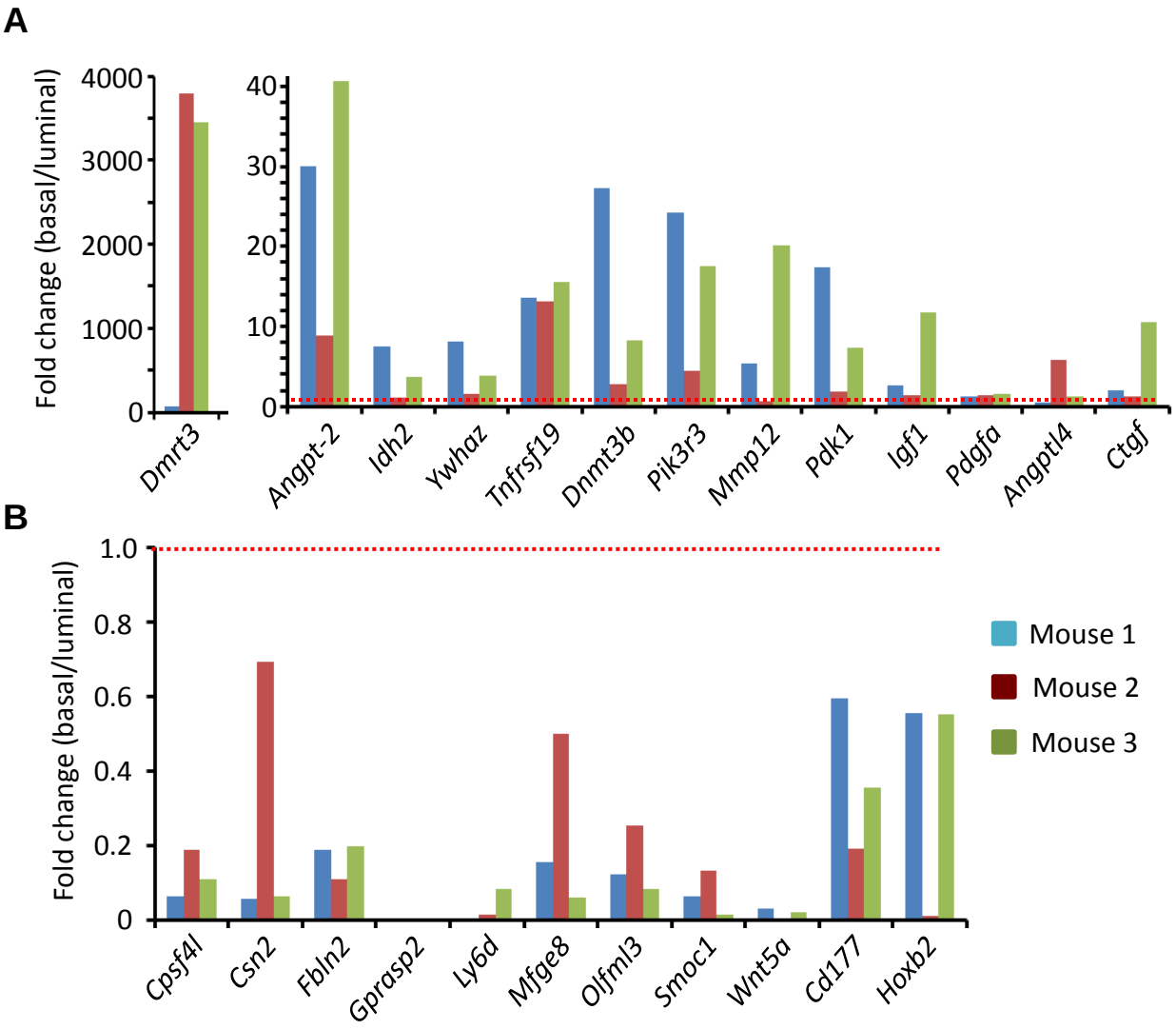
A
Fold change (basal/luminal)
4000
3000
2000
1000
0
40
30
20
10
0
Dmrt3
Angpt-2
Idh2
Ywhaz
Tnfrsf19
Dnmt3b
Pik3r3
Mmp12
Pdk1
Igf1
Pdgfa
Angptl4
Ctgf
B
Fold change (basal/luminal)
1.0
0.8
0.6
0.4
0.2
0
Cpsf4l
Csn2
Fbln2
Gprasp2
Ly6d
Mfge8
Olfml3
Smoc1
Wnt5a
Cd177
Hoxb2
Mouse 1
Mouse 2
Mouse 3

Figure S2

A

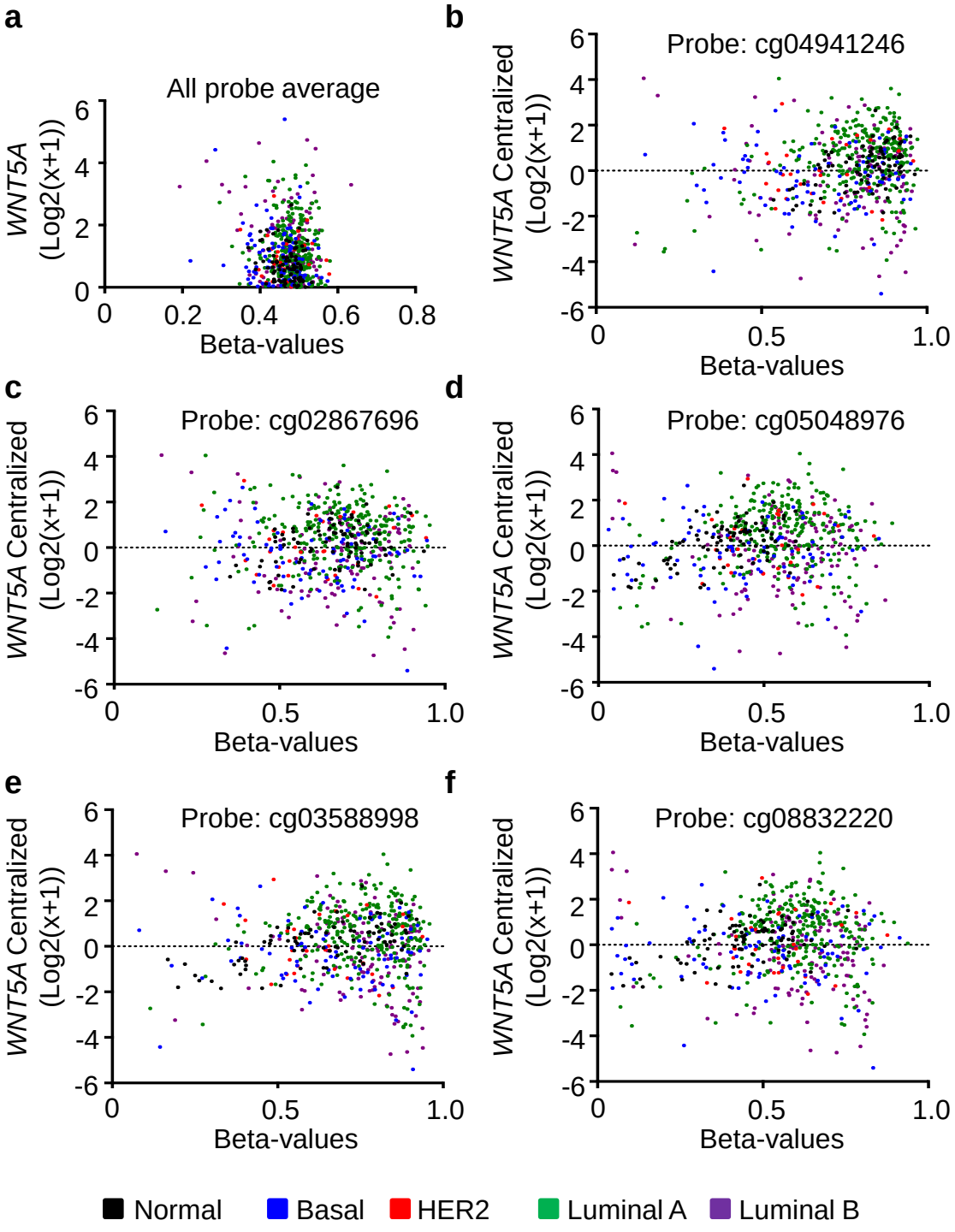
a
All probe average
WNT5A (Log2(x+1))
Beta-values
b
Probe: cg04941246
WNT5A Centralized (Log2(x+1))
Beta-values
c
Probe: cg02867696
d
Probe: cg05048976
e
Probe: cg03588998
f
Probe: cg08832220
Normal
Basal
HER2
Luminal A
Luminal B

Figure S2

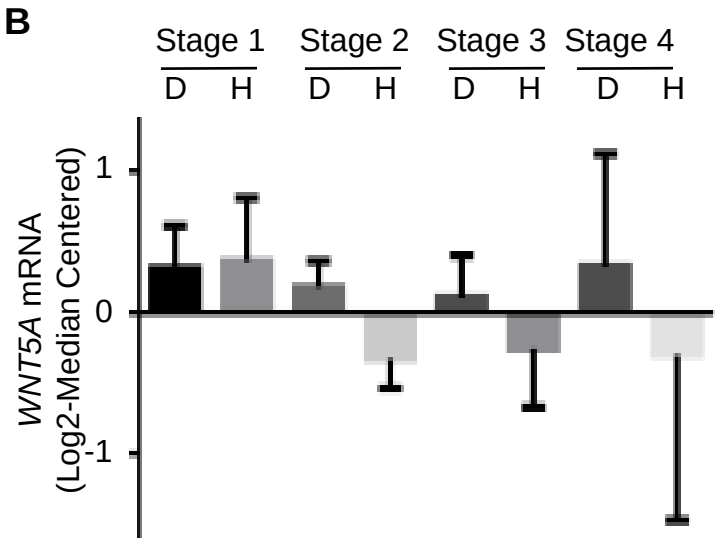
B
Stage 1
Stage 2
Stage 3
Stage 4
D H D H D H D H
WNT5A mRNA
(Log2-Median Centered)
1
0
-1

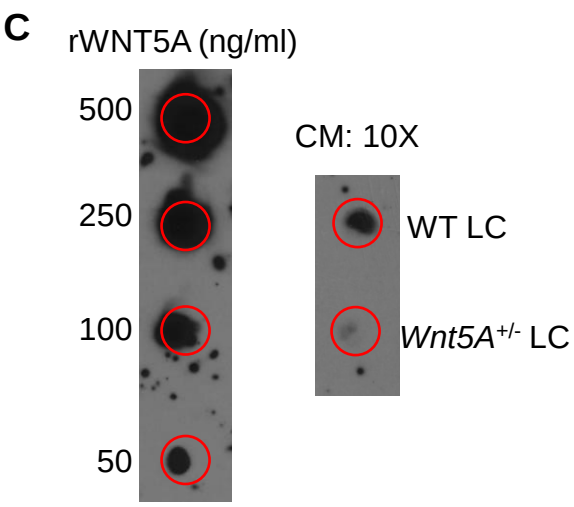
C
rWNT5A (ng/ml)
500
250
100
50
CM: 10X
WT LC
Wnt5A+/- LC

Figure S3

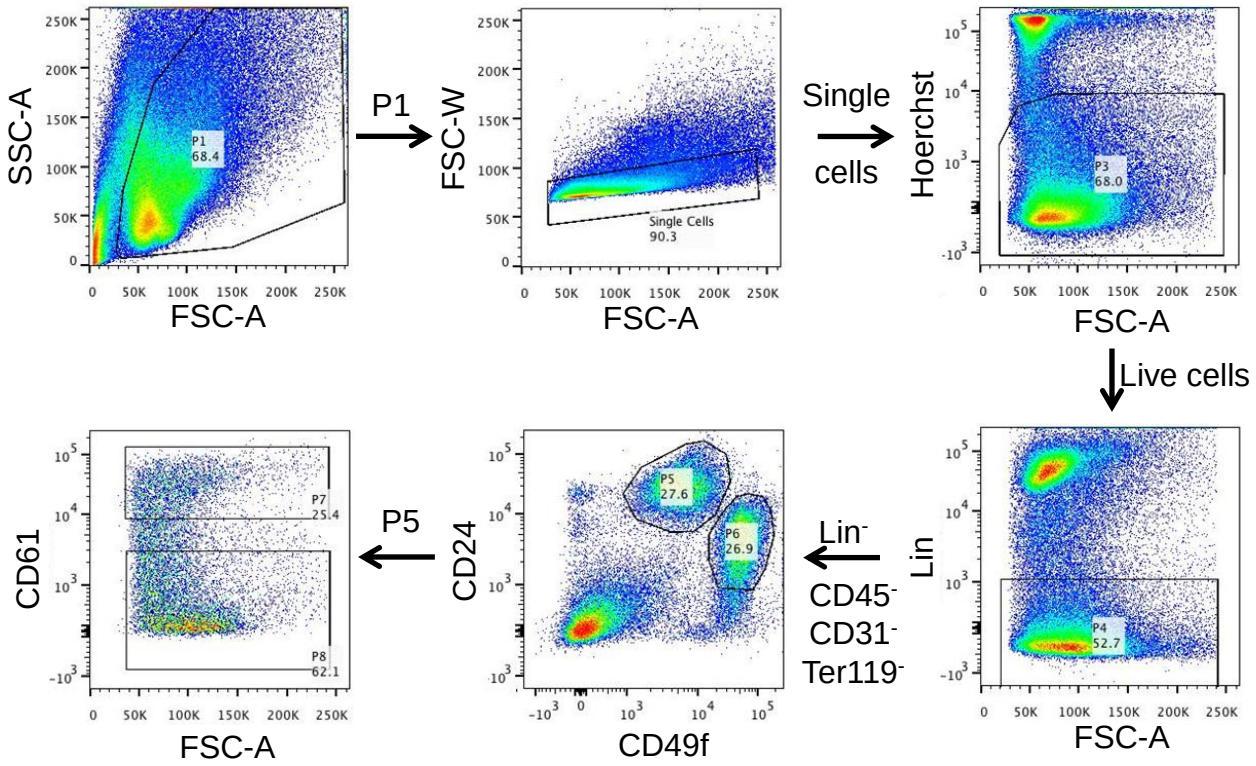
SSC-A
FSC-A
P1
68.4
P1
FSC-W
FSC-A
Single Cells
90.3
Single
cells
Hoerchst
FSC-A
P3
68.0
Live cells
Lin
FSC-A
P4
52.7
Lin-
CD45-
CD31-
Ter119-
CD24
CD49f
P5
27.6
P6
26.9
P5
CD61
FSC-A
P7
25.4
P8
62.1

Figure S4

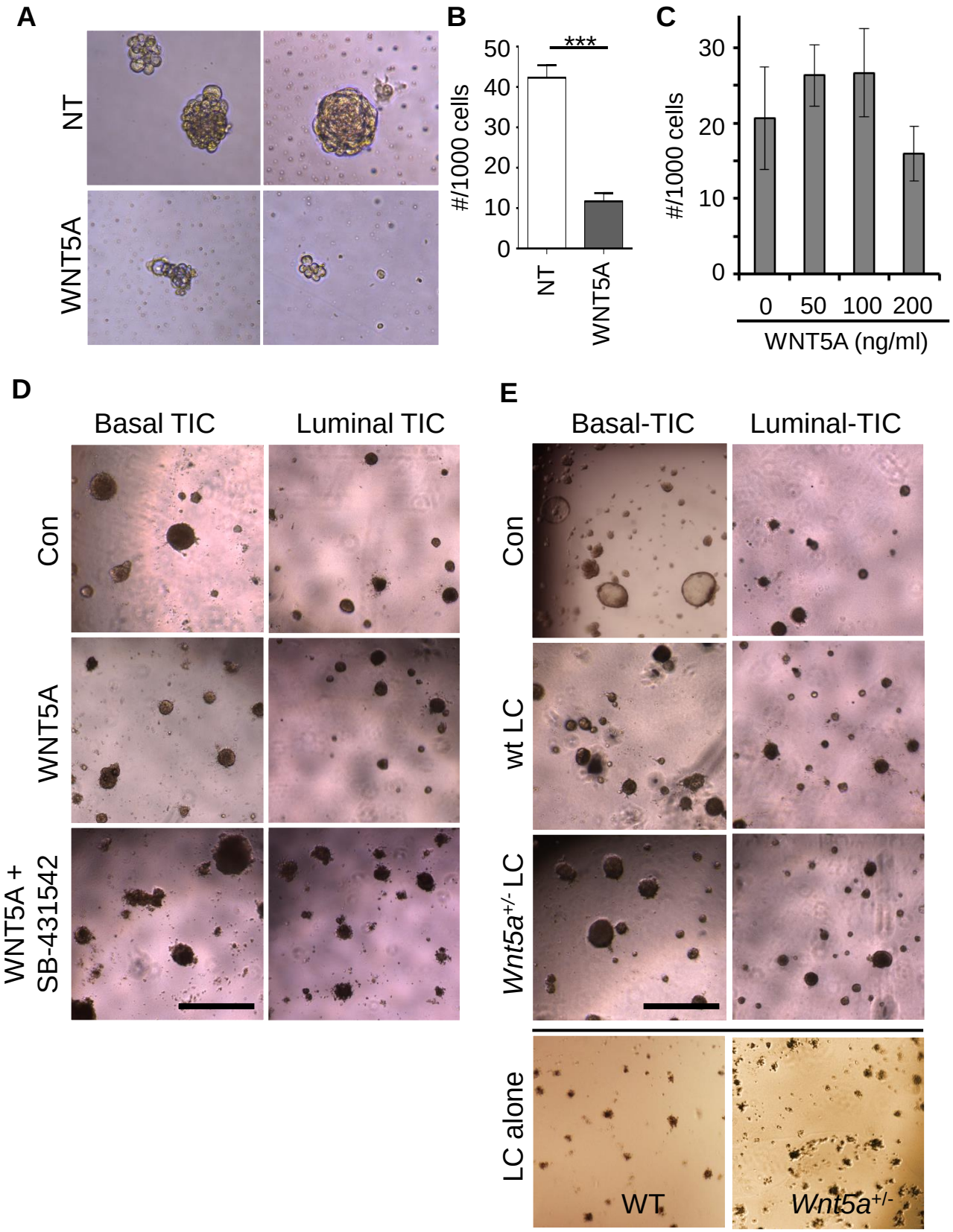
A
NT
WNT5A
B
***
#/1000 cells
50
40
30
20
10
0
NT
WNT5A
C
#/1000 cells
30
20
10
0
0
50
100
200
WNT5A (ng/ml)
D
Basal TIC
Luminal TIC
Con
WNT5A
WNT5A +
SB-431542
E
Basal-TIC
Luminal-TIC
Con
wt LC
Wnt5a+/- LC
LC alone
WT
Wnt5a+/-

Figure S4

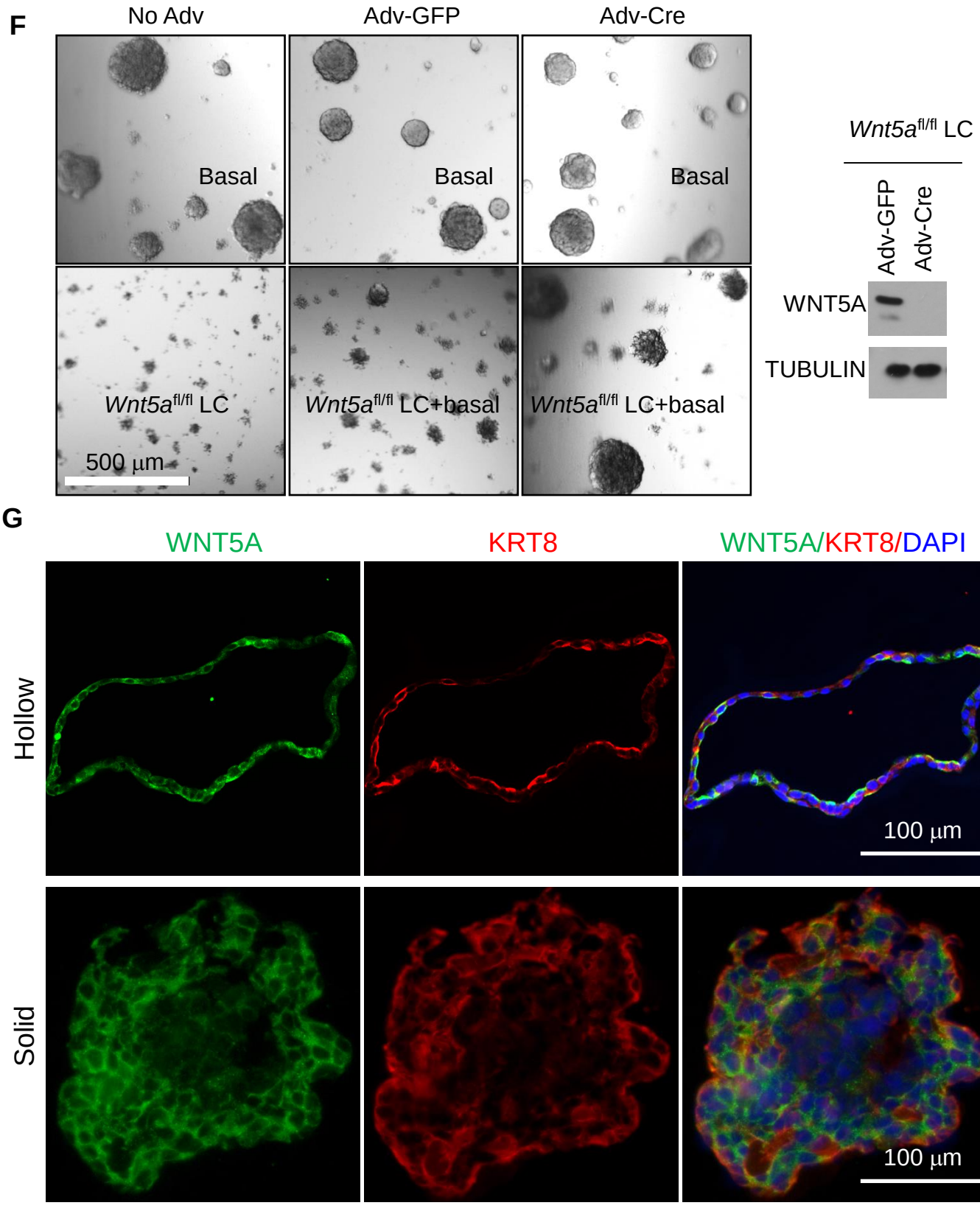
F
No Adv
Adv-GFP
Adv-Cre
Basal
Basal
Basal
Wnt5a fl/fl LC
Wnt5a fl/fl LC+basal
Wnt5a fl/fl LC+basal
500 μm
Wnt5a fl/fl LC
Adv-GFP
Adv-Cre
WNT5A
TUBULIN
G
WNT5A
KRT8
WNT5A/KRT8/DAPI
Hollow
Solid
100 μm
100 μm

Figure S5

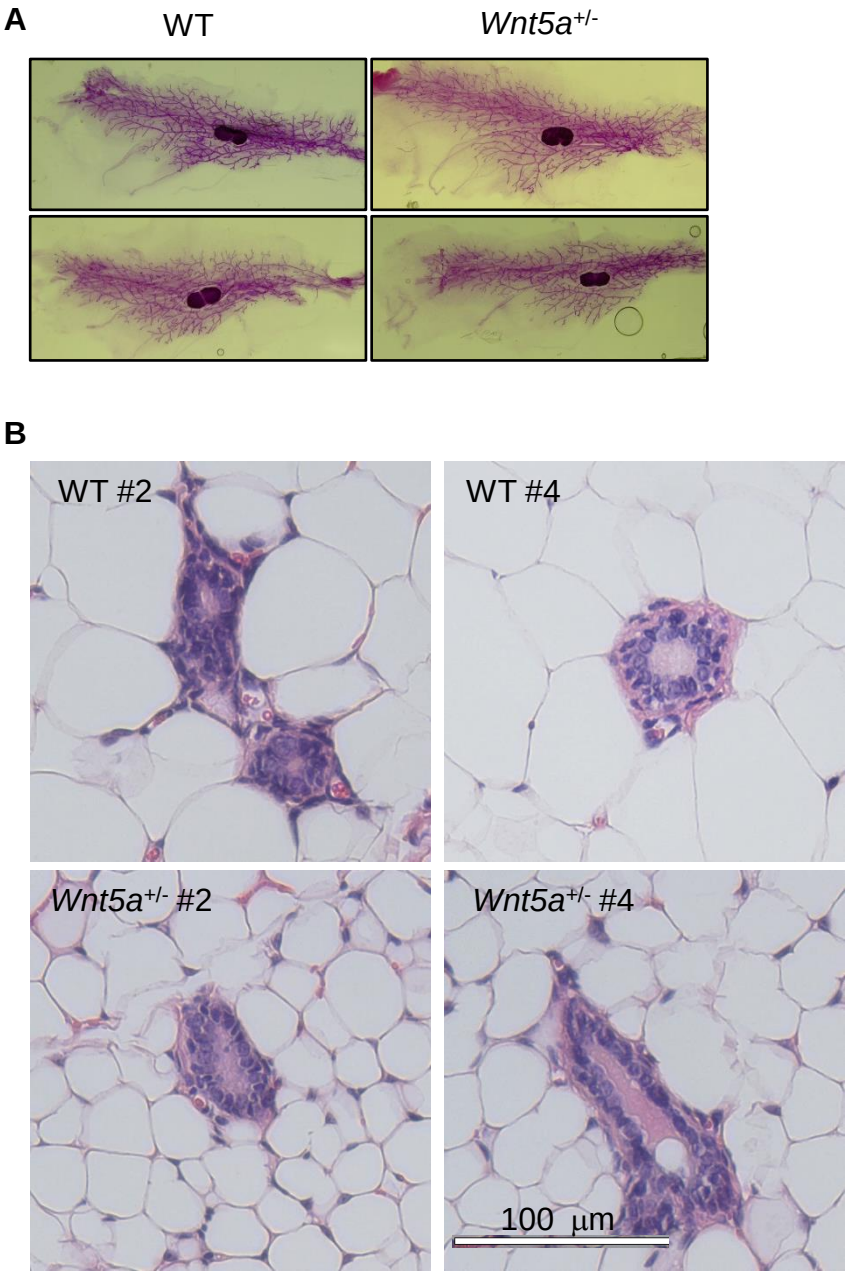

Figure S6

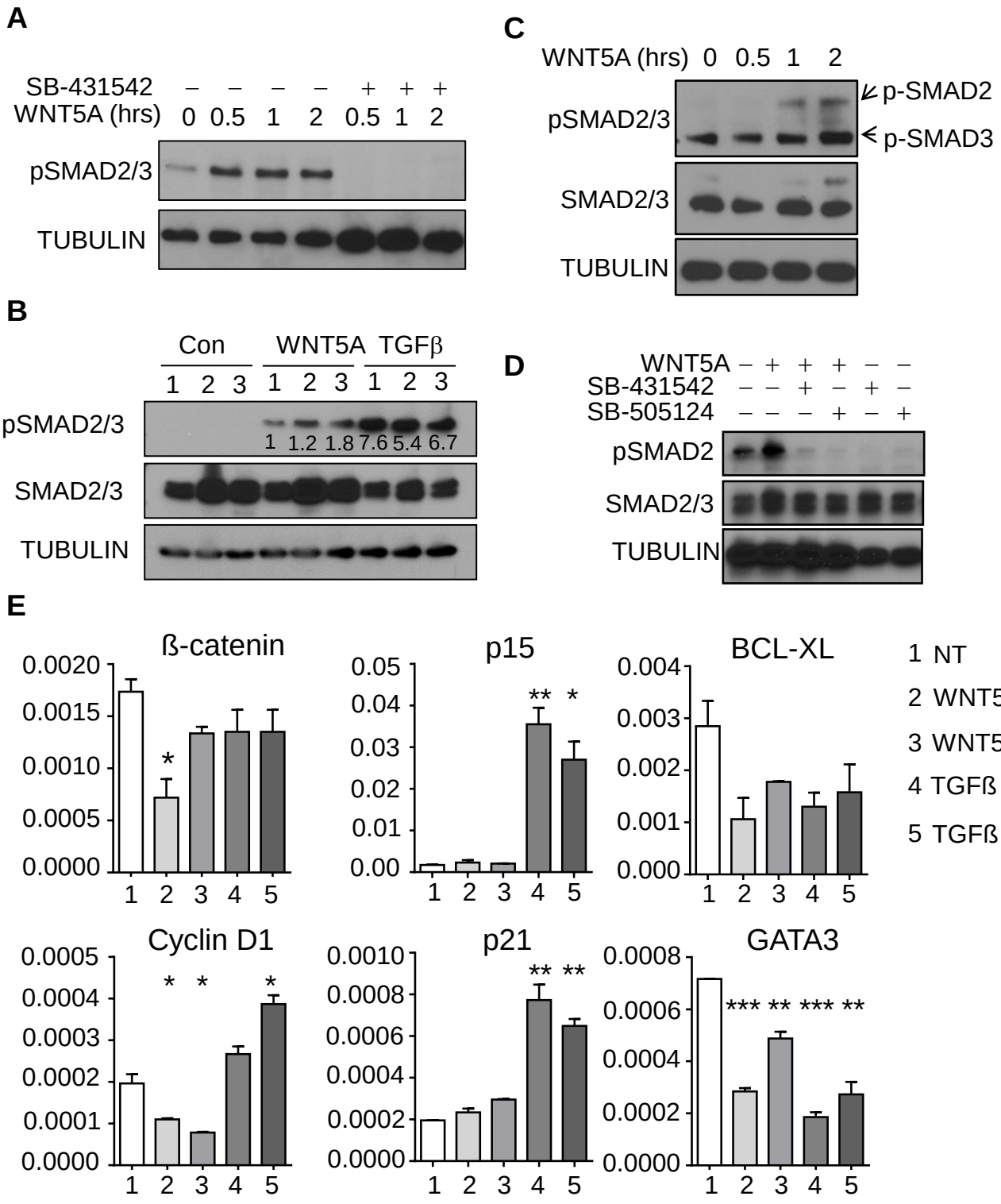
A
SB-431542 – – – – + + +
WNT5A (hrs) 0 0.5 1 2 0.5 1 2
pSMAD2/3
TUBULIN
B
Con
WNT5A
TGFβ
1 2 3 1 2 3 1 2 3
pSMAD2/3
1 1.2 1.8 7.6 5.4 6.7
SMAD2/3
TUBULIN
C
WNT5A (hrs) 0 0.5 1 2
pSMAD2/3
p-SMAD2
p-SMAD3
SMAD2/3
TUBULIN
D
WNT5A – + + + – –
SB-431542 – – + – + –
SB-505124 – – – + – +
pSMAD2
SMAD2/3
TUBULIN
E
ß-catenin
p15
BCL-XL
Cyclin D1
p21
GATA3
1 NT
2 WNT5A 4 hrs
3 WNT5A 8 hrs
4 TGFß 4 hrs
5 TGFß 8 hrs

Figure S7

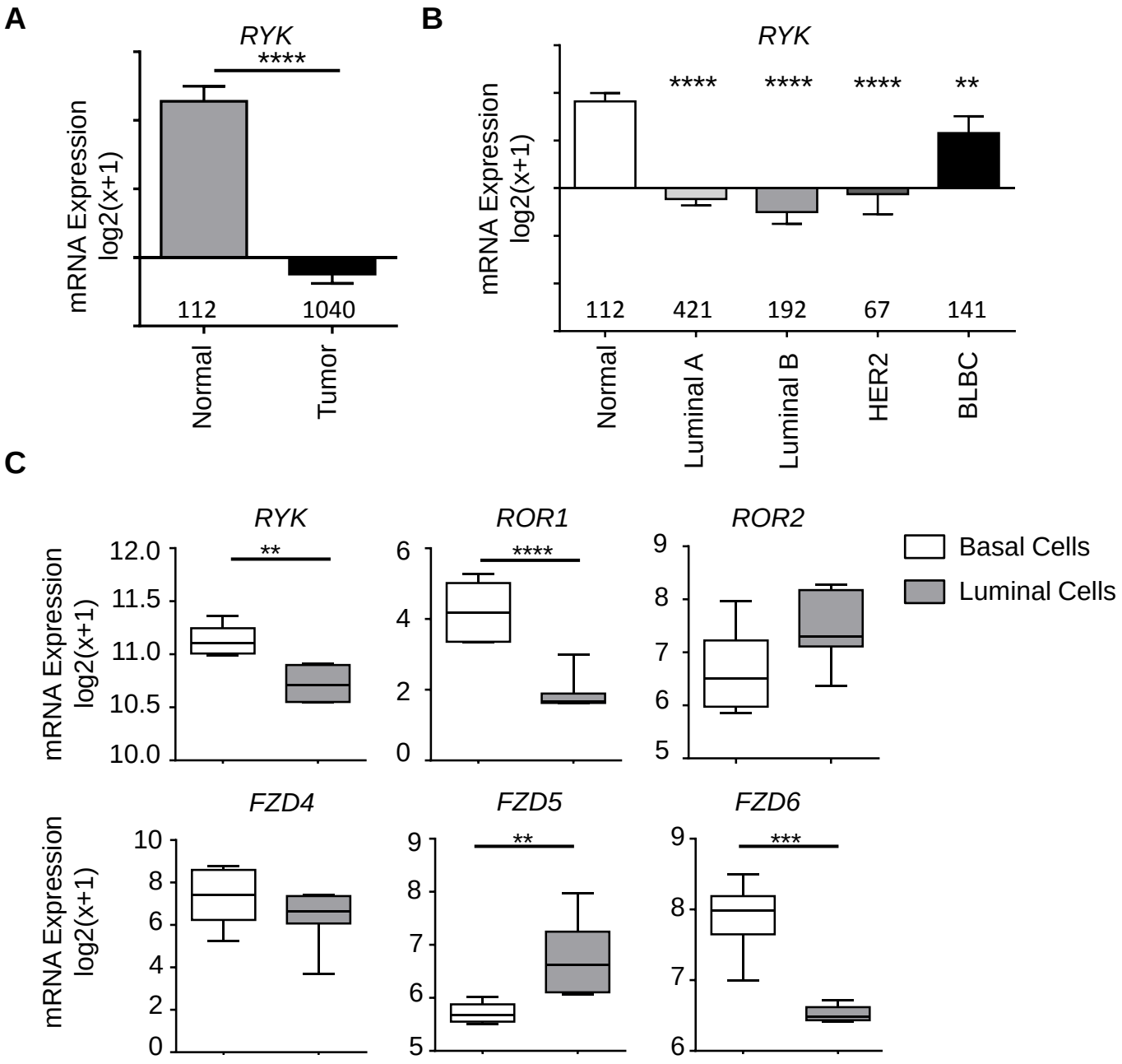
A
RYK
****
mRNA Expression
log2(x+1)
112
1040
Normal
Tumor
B
RYK
****
****
****
**
mRNA Expression
log2(x+1)
112
421
192
67
141
Normal
Luminal A
Luminal B
HER2
BLBC
C
RYK
**
ROR1
****
ROR2
Basal Cells
Luminal Cells
mRNA Expression
log2(x+1)
FZD4
FZD5
**
FZD6
***

Figure S7

D

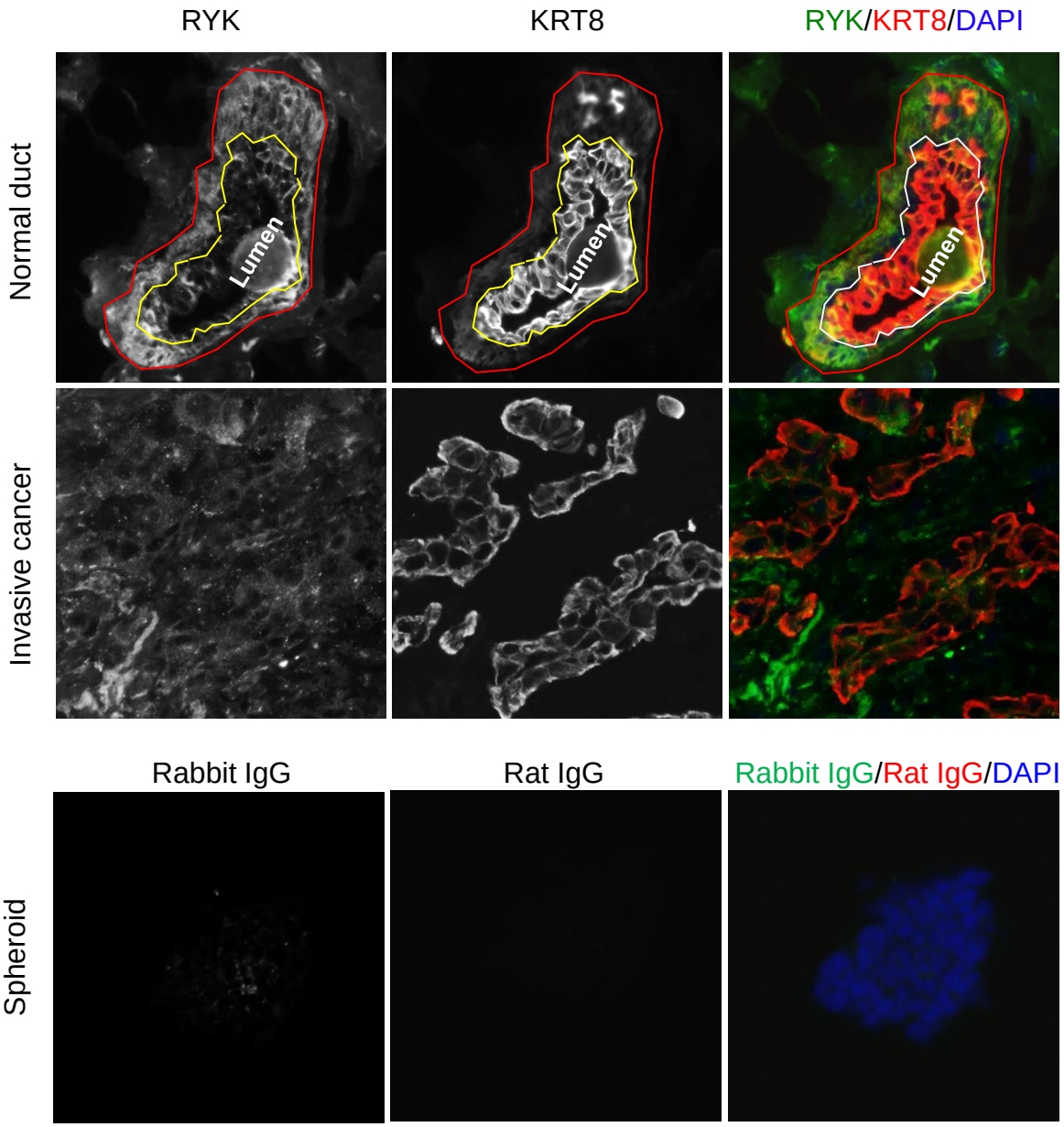
RYK
KRT8
RYK/KRT8/DAPI
Normal duct
Lumen
Lumen
Lumen
Invasive cancer
Rabbit IgG
Rat IgG
Rabbit IgG/Rat IgG/DAPI
Spheroid

Figure S8

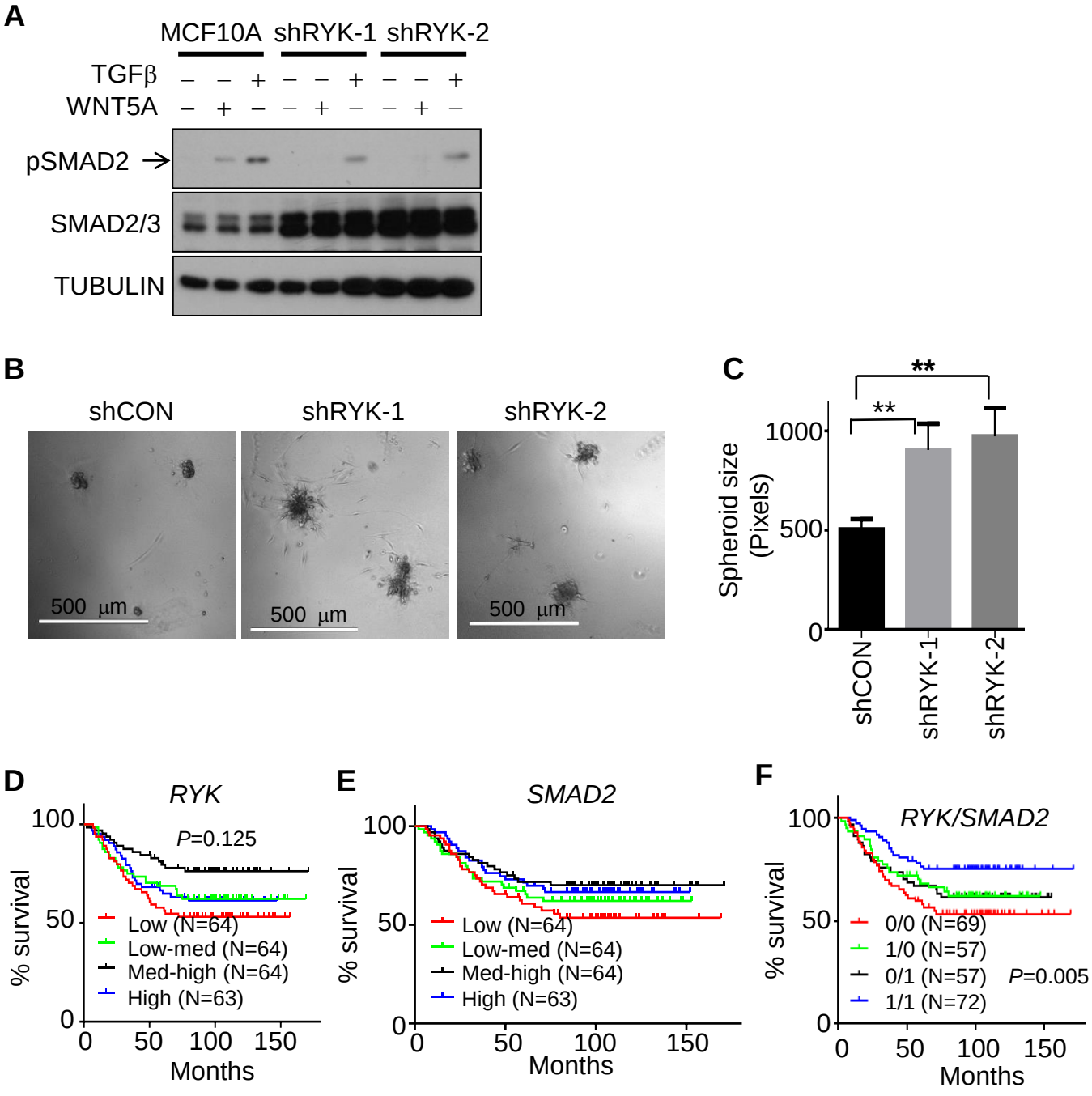
A
MCF10A
shRYK-1
shRYK-2
TGFβ
WNT5A
pSMAD2
SMAD2/3
TUBULIN
B
shCON
shRYK-1
shRYK-2
500 μm
C
Spheroid size (Pixels)
1000
500
0
**
**
shCON
shRYK-1
shRYK-2
D
RYK
P=0.125
% survival
100
50
0
Low (N=64)
Low-med (N=64)
Med-high (N=64)
High (N=63)
0
50
100
150
Months
E
SMAD2
% survival
Low (N=64)
Low-med (N=64)
Med-high (N=64)
High (N=63)
Months
F
RYK/SMAD2
% survival
0/0 (N=69)
1/0 (N=57)
0/1 (N=57)
1/1 (N=72)
P=0.005
Months

Figure S9